AIAA JOURNAL
Vol. 46, No. 8, August 2008

Lift on Stationary and Rotating Spheres Under Varying Flow and Surface Conditions

Jewel B. Barlow*
University of Maryland, College Park, Maryland 20742
and
Michael J. Domanski†
National Heart, Lung, and Blood Institute, Bethesda, Maryland 20892

DOI: 10.2514/1.28129

We examined the coefficient of lift for rotating and nonrotating spheres of varying surface texture under a variety of flight conditions. At Reynolds number less than 500,000 the direction of lift on a nonrotating polished sphere in a uniform flowfield is nonzero and in a direction that varies randomly with Reynolds number. However, once established, the direction and magnitude of lift appears to be stable over time at a particular Reynolds number. This phenomenon has not been reported previously. Additionally, the texture of a rotating sphere in a uniform flow can modulate direction and magnitude of lift generated by the spin. Although the expected direction of the net force on a spinning sphere is in a direction from the advancing to retreating surface ("Magnus effect"), in certain flight regimes the net force is in the opposite direction ("negative Magnus effect"). In this paper we present the first systematic wind-tunnel characterization of the flow parameters generating a negative Magnus effect on a sphere.

Nomenclature

A	=	reference area, $\pi d^2/4$
C_L	=	lift coefficient
d	=	diameter of sphere
L	=	lift, positive in the direction from the advancing side toward the retreating side
R_e	=	Reynolds number
r	=	radius of sphere
μ	=	viscosity of the air
ν	=	tangential to stream velocity ratio, $\omega r/V$
ρ	=	density of the air
ω	=	angular velocity of sphere

I. Introduction

THE fact that lift alters the trajectory of spinning spheres has long been recognized, dating at least as far back as the lifetime of Issac Newton [1–6]. Based on earlier flow separation on the advancing side, the lift generated by a spinning sphere in a uniform flowfield would be expected to be in a direction from the advancing side of the sphere toward the retreating side. The lift generated in this direction by a spinning sphere has been termed the "Magnus" effect. Indeed, the common experience with rotating seamed sports balls, such as baseballs, is that they curve in the direction predicted for the Magnus force.

A "negative" coefficient of lift (that is, in a direction opposite to that predicted for the Magnus effect) has been described for flows around rotating spheres and cylinders [7–10]. Prior studies of this so-called "negative Magnus effect" for rotating spheres provide limited quantitative data and do not fully define the flight conditions necessary for the phenomenon to occur.

In this study we examine three issues. First, we characterize flow about a nonrotating sphere as the Reynolds number R_e changes. Second, we determine the effect on the coefficient of lift C_L for rotating spheres caused by different flight conditions, and third, we examine the effect of surface texture on C_L under different flow conditions.

Received 1 October 2006; revision received 24 April 2007; accepted for publication 1 May 2007.

*Director, Glenn L. Martin Wind Tunnel, Aerospace Engineering Department, 3181 Martin Hall. Associate Fellow AIAA.
†Chief, Atherothrombosis and Coronary Artery Disease Branch.

II. Methods

A. Wind Tunnel

The experiments were conducted in the Glenn L. Martin Wind Tunnel at the University of Maryland, a closed return, solid wall wind tunnel with a test section height of 7.75 ft (2.36 m) and width of 11.04 ft. (3.37 m) with 10 in. (254 mm) filets. The area of the test section is 85.04 ft^2. The stream turbulence level is 0.21%, as measured by a hot wire anemometer with a corresponding turbulence factor of 1.05. Flow angularity in the central portion of the test section within 2 ft of the tunnel centerline is less than 0.1 deg.

B. Experimental Design

The spheres used in this study were stainless steel shells, 12 in. (304.8 mm) in diameter with a wall thickness of 0.125 in. (3.175 mm). One sphere was polished to a mirror finish. A second sphere had four 0.25 in. (6.35 mm) wide strips of aluminum tape arranged 90 deg apart on the sphere with five layers providing a height of 0.045 in. (1.14 mm) for a height-to-diameter ratio of 0.0037. A third sphere had a "mill" finish which was generated by a grinding operation to remove a weld seam bulge acquired during manufacture. The grinding marks were approximately 0.010 in. (0.025 mm) from valley to peak corresponding to a roughness height-to-diameter ratio of approximately 0.0008. The portion of the sphere surface in this condition was a strip approximately 2 in. (50.8 mm) wide, the center of which was the great circle in the plane that bisected the sphere and was perpendicular to the axis of rotation.

The spheres were mounted on a sting system with a motor drive so that they could be rotated at various rotational speeds about an axis perpendicular to the airstream. Figure 1 shows the arrangement looking downstream through the test section. The entire support structure was mounted to the main wind-tunnel balance which measures three force and three moment components. The main structure of the support system and the drive motor were shielded from the airstream. Fifteen inches (381 mm) of the support shaft nearest the sphere were not shielded so that measured aerodynamic force included the force on this segment of shaft. The mounting shaft was not permitted to rotate and the sphere was rotated by an attached

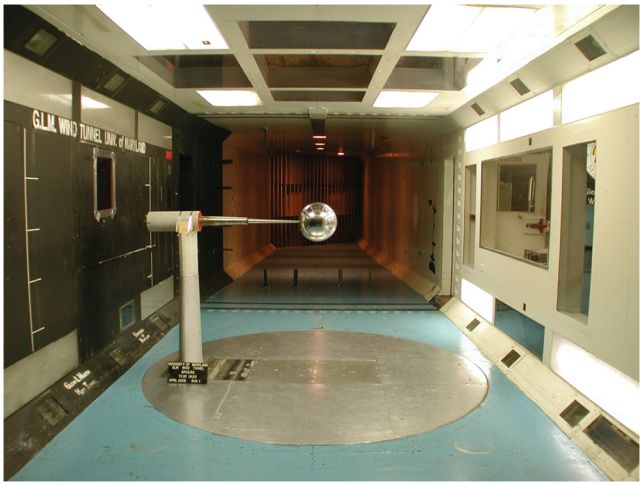

Fig. 1 Polished sphere in wind tunnel looking downstream.

internal shaft. Figure 1 shows the polished sphere from upstream in the wind tunnel.

To assess the forces on the exposed portion of the shaft, an "image" section of shaft was arranged to extend on the opposite side of the sphere as shown in Fig. 2. By making measurements with the image shaft section in place, and again after removing it, the incremental force associated with this section was obtained [11]. These measurements were then used to adjust the measurements of aerodynamic force on the sphere for the influence of the exposed shaft section in the standard run arrangement as shown in Fig. 1.

The data collected included the rotational speed of the spheres and the forces on the spheres obtained from the balance along with the wind-tunnel stream speed, temperature, and pressure. The rotational speed was set by varying the voltage to a direct current motor. Rotational speed was measured by a tachometer that was part of the motor and checked using a strobe light system. This provided rotational speed to within ± 1 rpm. The balance provided eight readings per second. Data samples were taken until the precision of the mean was less than 0.02 lb (0.089 N) for lift. This typically required 48 to 96 readings over 8 to 12 s. The precision of the mean for every value of lift coefficient reported in this paper was computed based on the assumption that the data samples are from a normally distributed population. The largest uncertainty of the precision of the mean for a value of the lift coefficient was 0.018. In almost all cases this uncertainty was less than 0.01. The blockage of the sphere and the mounting hardware in the tunnel gives a blockage correction using standard methods for the dynamic pressure of a little less than 1%.

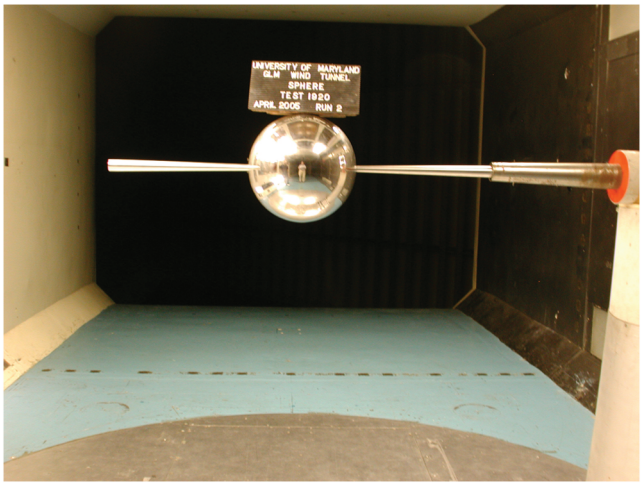

Fig. 2 The sphere with the "image" shaft section.

C. Data Collection

The rotational speed of each sphere was set at a sequence of values from zero to about 2500 rpm. The tunnel speed was set at a sequence of values from about 20 ft/s (6.1 m/s) to about 150 ft/s (45.7 m/s). Each run consisted of setting the sphere rotation rate and varying the air speed (referred to as a "sweep" for dynamic pressure in the run list), or setting the air speed and varying the sphere rotation rate (referred to as a sweep for rotation rate in the run list). The set of runs for which data are reported is shown in Table 1.

D. Data Analysis

The lift coefficient on a perfectly smooth sphere rotating and translating through a quiescent Newtonian fluid depends on the Reynolds number, the tangential-to-stream velocity ratio, nondimensional time, and Mach number. For the speeds in this study compressibility was negligible and Mach number was considered to be zero. The data reported here are time averages. Figure 3 shows C_L versus R_e for runs 1, 4, and 8 for the nonrotating polished sphere. Figure 4 shows C_L from runs 5, 6, 7, and 9–17. These are runs for the polished sphere over a range of nonzero rotation rates for a set of air speeds. Figure 5 shows C_L for runs 18, 19, and 21–25. These are runs of the milled surface sphere over a range of nonzero rotation rates for a set of air speeds. Figure 6 shows C_L data for runs 29 and 30. These are cases of the taped sphere over a range of rotation rates for two air speeds.

III. Results

A. Nonrotating Sphere ($\upsilon = 0$)

Figure 3 shows the relationship of C_L to R_e for a polished, nonrotating sphere and for a milled nonrotating sphere. Two distinct flow regimes were observed. Above a R_e of about 400,000, the coefficient of lift was essentially zero. Below 400,000, the direction of lift varied in an apparently random fashion within a run when speed was changed, but not with time once a speed was set. The magnitude of C_L, however, appeared, on multiple runs, to be strongly related to R_e and reproducible on multiple runs. With increasing R_e up to about 250,000, the magnitude of C_L increased and then declined to zero at R_e of about 400,000. The reproducibility of the data for the polished sphere was established by the collection of data over three distinct runs. There were fewer data for the milled surface nonrotating case, but the general pattern was the same as for the polished sphere.

B. Rotating Polished Sphere ($\upsilon > 0$)

Figure 4 shows the relationship of C_L to υ for the polished sphere over a range of R_e from $\sim$120,000 to $\sim$933,000. For R_e less than about 370,000, C_L became increasingly negative as υ increased, reaching a nadir at υ between 0.18 and 0.20 and then rising monotonically reaching zero at υ between 0.41 and 0.62 (Fig. 4). For the polished sphere, the minimum C_L (most negative) was similar for all R_e up to about 370,000. The value of υ at which C_L goes from negative to positive decreases with increasing R_e until, for R_e around 500,000, there is no longer any υ for which C_L was negative. An exception to this pattern occurred at R_e of 120,374. At all R_e greater than 500,000, C_L was a positive, monotonically increasing function of υ and for all υ greater than about 0.85, the C_L versus υ relationship was similar except, perhaps, at the lowest R_e of about 120,000.

C. Rotating Milled Sphere ($\upsilon > 0$)

Figure 5 shows the relationship of C_L to υ for the milled sphere over a range of R_e from $\sim$181,000 to $\sim$933,000. For R_e less than 500,000, C_L became increasingly negative as υ increased, reaching a nadir between 0.2 and 0.3 and then rising monotonically, reaching zero at υ between 0.3 and 0.75 (Fig. 5). Increasing R_e resulted in a less negative nadir and a reduction in the υ at which $C_L = 0$. For all R_e greater than 500,000, C_L was a positive, monotonically increasing function of the υ and the geometry of the C_L versus υ relationships were similar. Additionally, with increasing υ, the C_L versus υ relationship became essentially the same as the relationship obtained

Table 1 Run list with conditions for which data are reported

Run no.	Sphere rotation rate, rpm, approx.	Dynamic pressure, psf, Pa	Surface condition
1	0	0.41–36.85, 19.6–1764.6	Polished
4	0	0.41–6.32, 19.6–302.6	Polished
5	0–1500	6.39, 306	Polished
6	87–2800	16.37, 784	Polished
7	80	0.41–25.58, 6.32–1225.0	Polished
8	0	0.41–25.58, 6.32–1225.0	Polished
9	130	0.41–25.58, 6.32–1225.0	Polished
10	200	0.41–25.58, 6.32–1225.0	Polished
11	370	0.41–25.58, 6.32–1225.0	Polished
12	600	0.41–25.58, 6.32–1225.0	Polished
13	1000	0.41–25.58, 6.32–1225.0	Polished
14	1600	0.41–25.58, 6.32–1225.0	Polished
15	2000	0.41–25.58, 6.32–1225.0	Polished
17	2500	0.41–25.58, 6.32–1225.0	Polished
18	50	0.41–25.58, 6.32–1225.0	Milled
19	100	0.41–25.58, 6.32–1225.0	Milled
20	0	0.41–36.83, 19.6–1763.7	Milled
21	200	0.41–25.58, 6.32–1225.0	Milled
22	300	0.41–25.58, 6.32–1225.0	Milled
23	600	0.41–25.58, 6.32–1225.0	Milled
24	1000	0.41–25.58, 6.32–1225.0	Milled
25	2000	0.41–25.58, 6.32–1225.0	Milled
28	0	0.41–36.83, 6.32–1763.7	Taped
29	56–2500	2.30, 110	Taped
30	0–2500	6.39, 306	Taped

at R_e greater than 500,000. The value of υ at which this occurred decreased with increasing R_e (below 500,000).

D. Rotating Taped Sphere ($\upsilon > 0$)

Figure 6 shows the relationship of C_L to υ for the taped sphere for two values of R_e, ~284, 000 and ~461, 000 along with data for the polished and milled spheres at nearly the same values of R_e as for the taped sphere and also data for R_e at a slightly higher value of R_e. At both low R_e (284,000 where the polished and milled spheres produced negative C_L) and higher R_e (461,000 where C_L was transitional for the polished and milled spheres), C_L for the taped sphere was positive for all $\upsilon > 0$ and the C_L for both values of R_e was quantitatively similar at similar υ (Fig. 6). The values of C_L for the taped sphere were higher than those for the polished and milled spheres at all values of R_e and υ.

IV. Discussion

We explored the lift generated by a nonrotating polished sphere, and the effect of surface roughness on the lift generated by rotating spheres, in uniform, low turbulence flow. This is the first study to

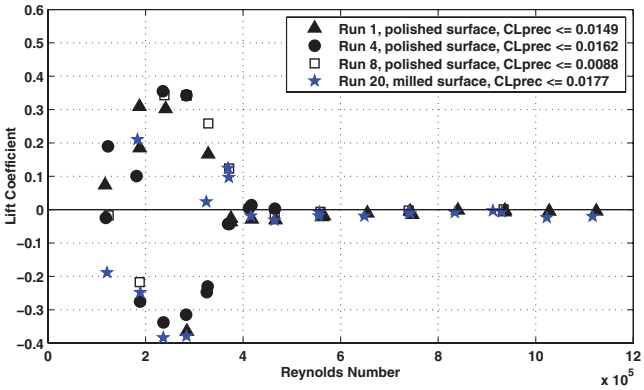

Fig. 3 C_L vs R_e for a nonrotating sphere.

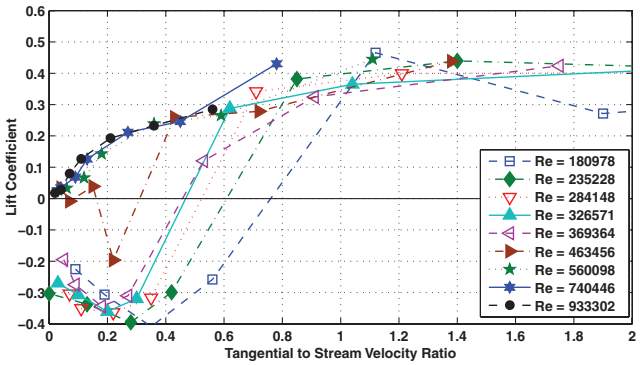

Fig. 5 C_L versus υ for a milled surface sphere.

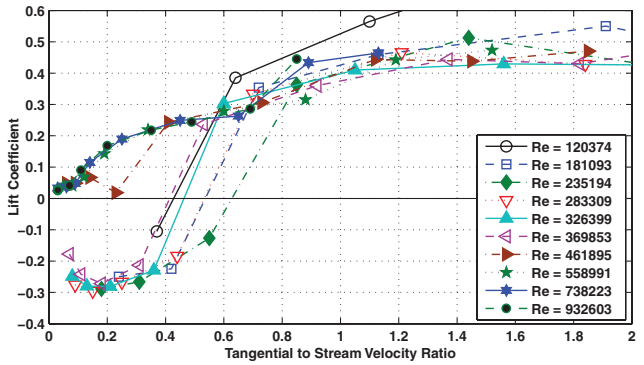

Fig. 4 C_L versus υ for a rotating polished sphere.

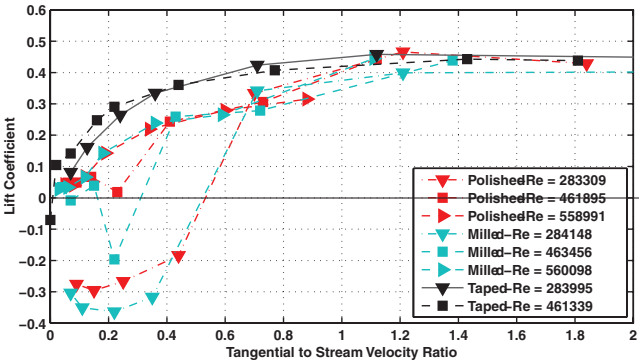

Fig. 6 C_L versus υ for three surface conditions.

report random variation with R_e and υ of temporally stable C_L. Further, it is the first systematic wind-tunnel study of the effect of surface roughness on the lift generated by rotating spheres.

A. Nonrotating Sphere

The zero net lift observed at R_e greater than 400,000 is the expected result for a perfect nonrotating sphere in a uniform flow. The nonzero lift observed at R_e less than 400,000 implies flow separation at different surface locations along the streamwise axis of the sphere. Small perturbations in the airstream and/or small deviations from spherical geometry could cause variation in the location of flow separation. Asymmetry of lift (and therefore the axial location of flow separation at the surface of the sphere) at R_e less than 400,000, but not above, suggests that the effect of small flow variations (perturbations) is attenuated as the total energy in the flow becomes large (with increasing R_e, or as noted later, at low υ).

An intriguing observation is the random variation of the direction of lift with changing Reynolds number, but not with time. This has not been reported previously. That is, although it is expected that the perturbations generating the changes in direction of lift vary randomly over time, the direction of lift did not change with time, once it was established at a particular Reynolds number. Once established, the flowfield appears to have been sufficiently stable so that the random perturbations were of insufficient magnitude to alter the location of flow separation. Further study of this phenomenon will be needed to fully understand the mechanism.

Although the direction of lift varied randomly at R_e less than 400,000, there appeared to be a pattern to the variation in magnitude. Specifically, the envelope of the magnitude of C_L appeared to increase, reaching a peak at a R_e of about 200,000 and then declining to zero at R_e of 400,000. The magnitude of generated lift would be a function of both the total energy in the flow and the location of flow separation. Flow energy increases monotonically with increasing R_e but C_L increases and then decreases with increasing R_e, suggesting that the difference in location of flow separation on opposite sides of the sphere (more correctly asymmetry of separation location along the surface) increases for R_e up to about 200,000 and then decreases. The explanation for the change in lift magnitude with Reynolds number is not clear.

B. Rotating Spheres

1. *Case 1: The Taped Sphere*

A reasonable starting point is to consider a situation in which the boundary layer is fully turbulent at the leading edge of the sphere as would be expected for the taped sphere. In this case, fluid moving over the advancing side would be slowed more by the frictional effect of the surface than on the retreating side, exposing it to a more adverse pressure gradient. This would result in earlier flow separation on the advancing side and a net pressure force (positive lift) in a direction from the advancing to the retreating side of the sphere. Indeed, it is precisely this behavior that was observed. At all R_e, the C_L for the taped sphere was unidirectional and increased in magnitude with increasing Reynolds number over the range of this experiment.

2. *Case 2: The Polished Sphere*

The behavior of the polished sphere was qualitatively different for R_e less than 500,000 and υ less than 0.75. In this regime, C_L was increasingly negative for υ up to 0.18 to 0.20 where it reached a minimum, and then rose monotonically with increasing υ, eventually becoming positive (crossing through zero for υ between 0.4 and 0.6), and continuing to rise monotonically. This demonstrates the so-called negative Magnus effect [7–10].

Such behavior would be caused by a more forward flow separation on the retreating than on the advancing side. An explanation for this behavior on cylinders has been offered by Fletcher [8]. For cylinders operating at sufficiently high Reynolds number, the boundary layer transitions to turbulence before separating. In this case, the adverse pressure gradient would be less on the retreating side resulting in more aft separation than on the advancing side. For R_e less than 500,000, however, Fletcher suggested that separation occurs before transition to turbulence. In this situation, the transition of the boundary layer would occur sufficiently close to the separation point on the advancing side to permit boundary layer reattachment. On the retreating surface, however, transition would occur later and with the boundary layer sufficiently removed from the cylinder to prevent reattachment. Although we were working with spheres and three-dimensional flow, this mechanism would explain our observations. The gradual decrease in the magnitude of the negative lift with increasing υ could be explained by a gradual movement of the transition zone closer to the point of laminar separation with increasingly forward reattachment until laminar boundary layer separation no longer occurred.

3. *Case 3: The Milled Sphere*

Qualitatively, C_L for the milled sphere behaved in a manner similar to the smooth sphere. The nadir of the C_L was somewhat more negative than for the smooth sphere, suggesting some quantitative differences in the relative degree of boundary layer turbulence at a given υ compared to the polished sphere.

C. Other Studies

Observation of lift generated by a spinning ball has been attributed to Magnus [5]. The impact of surface roughness has also received some limited examination. Macoll [2] has been credited with the first observation of negative ("lift in a direction from the retreating to the advancing surface") lift on a spinning sphere. He studied the C_L for 6-in. diam spheres rotating in a wind tunnel. The reported C_L was negative for low υ, the so-called negative Magnus effect, and then became positive at higher υ. There are very limited data.

Davies [3] reported data on smooth and dimpled golf balls dropped through airflow perpendicular to the axis of spin and used measured landing points to assess the lift generated on the ball. Below an equatorial speed of 2100 ft/ min, the lift was negative for the smooth balls. Lift was positive at higher equatorial speed.

Brown [12] reported C_L for a 3.36-in. diam sphere studied in a wind tunnel. He found a negative C_L at low υ that became zero at υ 0.1 to 0.5 (generally comparable to our findings) and positive lift at higher υ.

Briggs [4] found a negative Magnus effect for smooth spheres in certain flight regimes and a uniformly positive lift for baseballs.

D. Limitations

The experimental setup for this study permitted measurement of force only in directions perpendicular to the airflow and to the axis of the sting attaching the sphere to the balance. For the nonrotating sphere, it is virtually certain that there is variation of flow separation over the surface of the sphere that results in forces out of the plane of our measurement. Further, we do not have measurements of pressure over the surface of the spheres nor do we systematically visualize the flow to determine the specific location of flow separation.

E. Future Directions

A better understanding of the physics underlying the phenomena observed would be useful. For the nonrotating sphere, a better understanding and quantification of the perturbations that result in the random direction of lift would be an advance. Why these perturbations have the effect that they do at lower Reynolds number, but not above a certain Reynolds number, could be examined. The reason for the stability of the direction and magnitude of the lift, once established, needs to be better understood.

The distribution and magnitude of "out-of-plane" forces on the rotating spheres requires study. Further, the actual distribution of pressures and the location of flow separation across the surface of spheres under different flow conditions and with different surface roughness requires further study.

Finally, studies of the effect of rotation about axes not perpendicular to the flow direction are of interest.

V. Conclusions

1) For R_e less than 500,000, the lift on a nonrotating sphere in a uniform flowfield is nonzero and the direction varies randomly with the Reynolds number. However, once established, the direction and magnitude of lift appears to be stable over time at a particular Reynolds number. This phenomenon has not been reported previously.

2) This study characterized how the texture of the surface of a rotating sphere in a uniform flow can modulate direction, as well as magnitude, of lift generated by the spin.

3) This is the first systematic wind-tunnel characterization of the effect of three-dimensional flow over spheres in flight regimes generating the so-called negative Magnus effect.

References

[1] Newton, I., "New Theory of Light and Colors," *Philosophical Transactions of the Royal Society of London*, Vol. 6, 1671, pp. 3075–3087.

[2] Macoll, J., "Aerodynamics of a Spinning Sphere," *Journal of the Royal Aeronautical Society*, Vol. 28, 1928, pp. 777–798.

[3] Davies, J., "The Aerodynamics of Golf Balls," *Journal of Applied Physics*, Vol. 20, No. 9, 1949, pp. 821–828. doi:10.1063/1.1698540

[4] Briggs, L., "Effect of Spin and Speed on the Lateral Deflection (Curve) of a Baseball and the Magnus Effect for Smooth Spheres," *American Journal of Physics*, Vol. 27, No. 8, 1959, pp. 589–596. doi:10.1119/1.1934921

[5] Magnus, G., "On the Deviation of Projectiles and on a Remarkable Phenomenon of Rotating Bodies," *Memoirs of the Royal Academy of Berlin*, 1852. English translation in *Scientific Memoirs*, selected from the Transactions of Foreign Academies of Science and Learned Societies, edited by J. Tyndall and W. Francis, Taylor, London, 1853, p. 210.

[6] Rayleigh, L., "On the Irregular Flight of a Tennis Ball," *Scientific Papers*, Dover Publications, New York, 1964, Vol. 1, p. 344.

[7] Krahn, E., "Negative Magnus Force," *Journal of the Aeronautical Sciences*, Vol. 23, April 1956, pp. 377–378.

[8] Fletcher, C., "Negative Magnus Forces in the Critical Reynolds Number Regime," *Journal of Aircraft*, Vol. 9, No. 12, 1972, pp. 826–833.

[9] Swanson, W., "An Experimental Investigation of the Magnus Effect," Case Institute of Technology, Cleveland, OH, Final Report, OOR Project 1082, Dec. 1956.

[10] Griffiths, R., and Ma, C., "Differential Boundary-Layer Separation Effects in the Flow Over a Rotating Cylinder," *Journal of the Royal Aeronautical Society*, Vol. 73, 1969, pp. 524–526.

[11] Barlow, J. B., Rae, W. H., and Pope, A., *Low-Speed Wind Tunnel Testing*, Wiley, New York, 1999, pp. 271–280.

[12] Brown, F. N. M., "See the Wind Blow," Department of Aerospace and Mechanical Engineering, Univ. of Notre Dame, South Bend, IN, 1971.

F. Coton
Associate Editor